

Performance of a Flat Sheet Scintillator Calorimeter Prototype*

Eric Scott and Scott Teige
Department of Physics
Indiana University, Bloomington, IN 47405

Abstract

The construction and performance of a one meter long calorimeter prototype is discussed. This prototype is based on a laminated lead sheet-thin scintillator design. Mechanical measurements, observations on manufacturability and the response of the device to cosmic rays are presented.

Submitted to TJNAF

*Work supported by Department of Energy contract DE-FG02-91ER40661 and Thomas Jefferson National Accelerator Facility

1 Introduction

Many calorimeters have been built using lead/scintillating fiber (SciFi) construction. A selective overview of such devices can be found in [?]-[?] The GlueX collaboration is actively pursuing this technology for the barrel calorimeter [?].

Electromagnetic SciFi calorimeters are capable of achieving good energy and position resolution, at least as good as lead glass calorimeters. This performance is due to the high ($\approx 50\%$) volume fraction of active material in typical designs. Large calorimeters have been built [?] and operated in environments similar to that of GlueX. A disadvantage of the SciFi design is the large amount of custom tooling and skilled labor required to assemble such devices.

To achieve the good performance characteristics of the SciFi design and minimize the need for custom tooling and skilled labor, the GlueX collaboration proposed to study a prototype module based on laminated sheets of lead and scintillator that maintained the large active material fraction characteristic of previous SciFi designs. Presented here are the results of these studies.

2 Construction

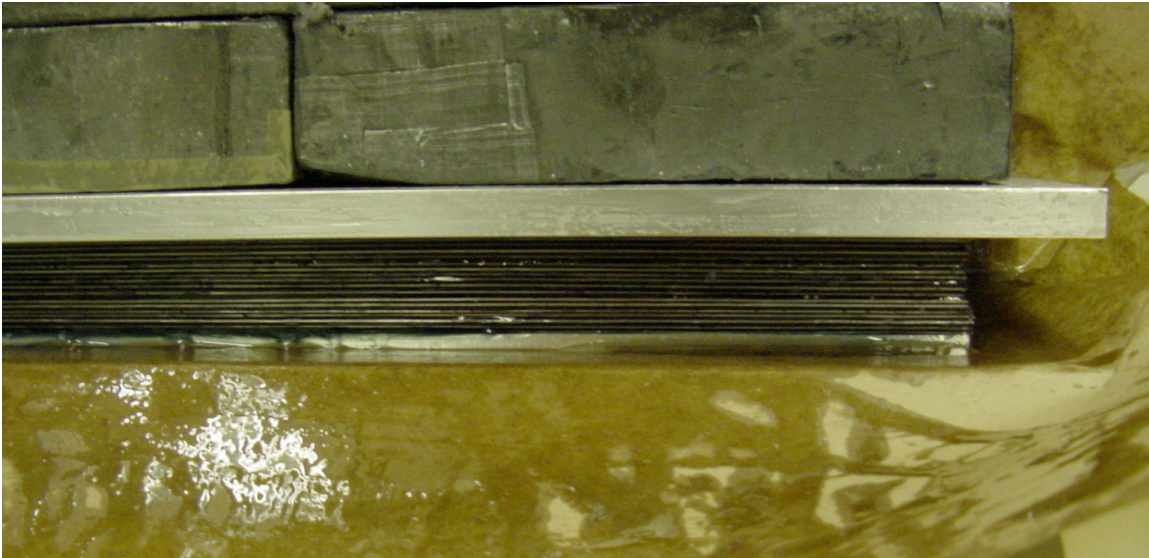


Figure 1: The glued 1 meter prototype under construction. Visible in the center are the alternating layers of lead and scintillator. These layers are glued on the bottom to a 0.25 *in* layer of aluminum for stability. On top is a sheet of aluminum and lead bricks to compress the stack while the glue cures.

A one meter long, $\approx 30\text{mm}$ thick prototype calorimeter element was built by laminating 16 sheets of nominal one *mm* thick Eljen type EJ200 scintillator between 17 sheets of one *mm* thick lead.

Bicron type 600 optical cement was used to bond the laminations together. The bottom sheet of lead was bonded to 0.25 *in* aluminum plate for structural strength. The stack was pressed under 400 pounds of lead bricks to compress the lamination and exclude air pockets. Figure ?? shows the stack under compression. After the optical cement had cured, the edges were machined flat and square.

3 Manufacturing Issues

The construction of the prototype proceeded without difficulty. A single technician was able to assemble the stack unassisted in less than 8 hours. A small jig, to assure a square edge of the stack was the only special tooling required. The machining of the edges was performed on ordinary machine shop tools. Larger, somewhat more unusual machines would be required for a full size module, but such facilities are readily available.

Manufacturing of the scintillator presented more serious difficulties. The order placed with Eljen Inc. specified a length of 1000 *mm*, a width of 100 *mm* and a thickness of 1.0 ± 0.1 *mm*. The sheets were to be cast on glass and the edges diamond machined. The "as cast" surfaces were the largest surfaces of the sheet. These surfaces are where most of the internal reflections that transmit the scintillation light occur. This casting technique gives the best surface finish achievable and is widely used in scintillator manufacturing.

The length and width tolerances were unimportant since the finished lamination would be machined to its final dimensions but the thickness tolerance was specified since this dimension would determine the final thickness of the module. During manufacturing we were informed by the manufacturer that the meeting the thickness tolerance specification would be problematic. It was decided to accept the sheets manufactured up to that time and measure the thickness variation achieved. A total of 14 months was required to manufacture the scintillator sheets. We were also informed by the manufacturer that extending the sheets to 4 meters (as required for the GlueX Barrel Calorimeter) was outside their capabilities.

The thickness of each sheet was measured at 5 places along its length. Table ?? shows the results of those measurements. No single sheet achieved the specified thickness tolerance. Variations of up to 40% were observed within a single sheet. One sheet was so thin that it cracked when the protective coating was removed.

Table 1: Measured scintillator thickness, millimeters

Pos.	1	2	3	4	5	Average
	0.95	1.05	1.03	1.07	0.80	0.98
	0.83	1.18	0.95	0.95	1.08	1.00
	0.98	0.93	0.84	1.06	1.01	0.96
	0.79	0.87	0.84	1.12	1.05	0.93
	0.95	0.91	0.91	0.96	0.89	0.92
	0.98	0.72	0.47	0.86	0.98	0.80
	1.09	1.26	1.26	1.48	1.10	1.24
	0.79	1.04	0.93	0.84	0.84	0.89
	0.76	0.79	0.96	1.00	0.78	0.86
	0.85	0.92	1.11	0.99	0.89	0.95
	0.88	0.94	1.05	0.98	0.91	0.95
	0.89	0.90	0.86	0.70	0.75	0.82
	0.81	1.09	1.07	1.06	0.91	0.99
	0.66	0.92	1.09	0.91	0.82	0.88
	0.60	0.96	1.03	0.89	0.74	0.84
	0.93	0.86	0.92	0.90	0.74	0.87
	1.00	0.85	0.88	0.92	0.85	0.90
	0.73	0.67	0.72	0.87	0.82	0.76
	0.63	0.73	0.75	0.82	0.72	0.73
	0.65	0.76	0.79	0.78	0.67	0.73
	0.55	0.53	0.61	0.72	0.61	0.60
	0.58	0.58	0.59	0.64	0.73	0.62
	0.87	0.84	0.92	0.97	0.97	0.91
	0.70	0.62	0.69	0.80	0.86	0.73
	0.59	0.88	0.98	0.90	0.75	0.82
	0.88	1.07	1.50	1.71	0.97	1.23
	0.85	1.53	1.65	1.47	0.73	1.25
	0.68	0.83	1.13	0.91	0.63	0.84
	0.87	1.08	1.12	1.15	0.98	1.04
	0.82	0.95	0.89	1.04	0.93	0.93
	0.70	0.87	0.95	0.77	0.59	0.78
	0.64	0.98	1.02	0.95	0.69	0.86

4 Performance

4.1 General technique

Because of the observed variations in thickness of the scintillator there was concern as to the ability of the sheets to transmit light by total internal reflection. Changes in thickness imply the surfaces are non-parallel and a photon propagating down the sheet encounters the surface at changing angles. These changes in angle of incidence can cause losses due to transmission across the surface of the sheet.

To address this concern, half of the scintillator sheets were reserved for study without bonding to lead sheets. The light yield due to a cosmic ray from a stack of these unbonded sheets was investigated and used as a basis of comparison for the observed light output of the prototype.

The prototype was placed in a light-tight enclosure (see figure ??). Phillips XP2020 phototubes were bonded with optical grease to each end of the module. Above and below the module were placed two 1 *in* square scintillators forming a cosmic ray telescope. A coincidence of top and bottom elements of the telescope served as the trigger for the tests. The output of the phototubes was digitized by custom made analog to digital converters (ADCs) previously used for Brookhaven National Lab experiment 852.

The remaining unglued sheets were stacked and clamped together between sheets of lead. When the unglued stack was tested, the glued prototype was removed and replaced with the unglued stack. This arrangement insured that the illumination of the unglued stack and the prototype was identical. For further ease of comparison, the same phototubes used on the glued stack were moved from the prototype to the unglued stack when comparison measurements were made. The tubes were operated at identical voltages and the same data acquisition channels were used.

The pedestal values of the two ADC channels was determined by a fit to the observed pedestal distribution. Figure ?? shows one of the channels and the fit. The pedestal width (≈ 1 channel) is small compared to other observed distributions (described below) and is neglected in the subsequent analysis.

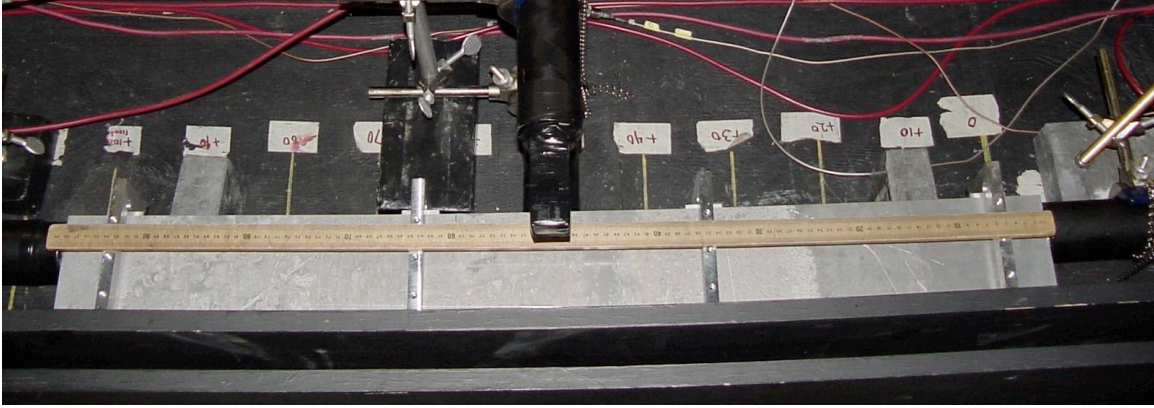


Figure 2: The finished unglued stack in the light tight enclosure. On the ends are visible the XP2020 phototubes. Near the center one of the trigger scintillators and its phototube can be seen. Not visible in the photo is the second trigger scintillator, located under the module. The apparent curvature of the module is an artifact of the camera optics, the actual module is straight to within one eighth of an inch.

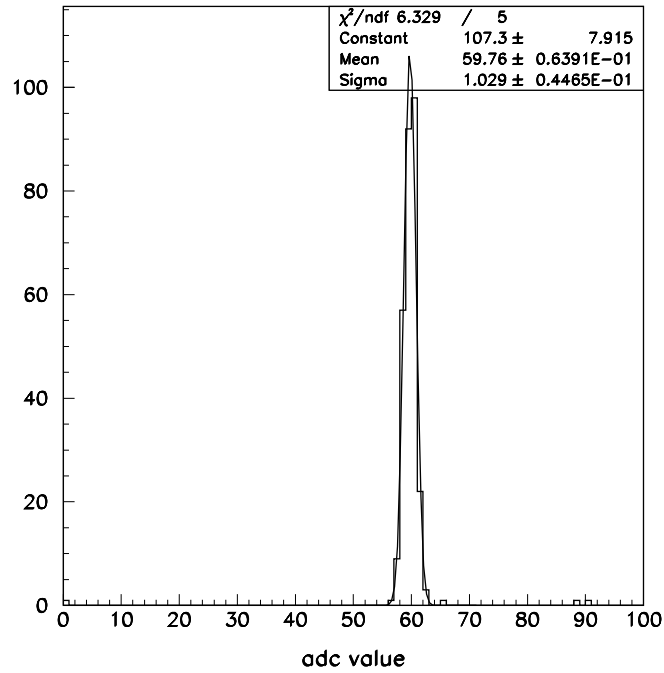


Figure 3: A typical ADC pedestal

4.2 Photoelectron yield

To determine the photoelectron yield from a minimum ionizing particle for the unglued stack the trigger scintillators were placed at the center of the stack and data accumulated. A typical ADC spectrum from one of the ends of the stack is shown in figure ???. The number of photoelectrons was determined by

$$\frac{\mu}{\sigma} = \frac{N}{\sqrt{N}} \quad (1)$$

where μ (P_2 in the figures) and σ (P_3) characterize the mean and width of the observed pulse height distributions. σ and μ were obtained by fitting

$$\frac{dN}{dx} = P_1 \exp \left[-\frac{1}{2} \left(\lambda + e^{-\lambda} \right) \right] \quad (2)$$

with

$$\lambda = \frac{x - \mu}{\sigma} \quad (3)$$

to the observed spectra. The values obtained from these fits gave yields of 25.2 and 29.9 photoelectrons from the two ends of the unglued stack. Equation ??? is an approximation to the Landau distribution.

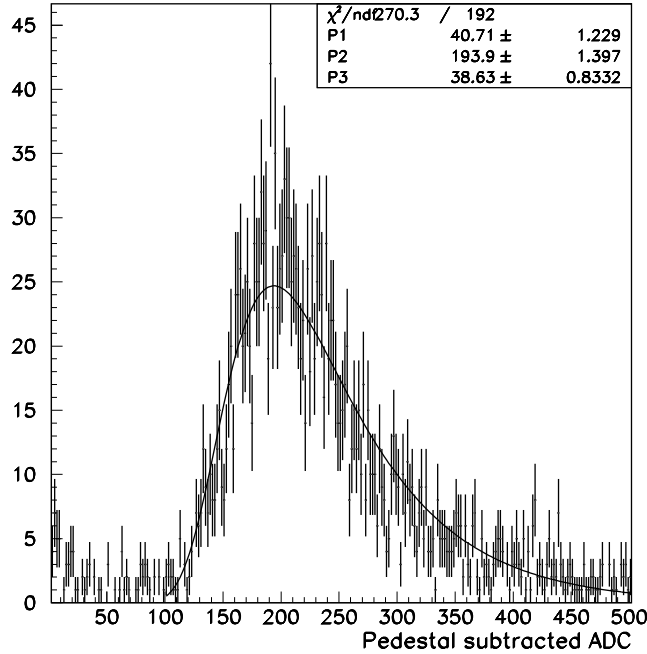


Figure 4: A typical ADC spectrum from the unglued scintillator stack. The curve is a fit to eqn ???.

The observed ADC pulse height distribution from one of the prototype phototubes is shown in figure ???. The data for this spectrum was acquired with an identical trigger and identical phototubes operated at identical voltages as for the unglued stack. Since the gain of the phototubes was

unchanged, the ratio of means and the known number of photoelectrons observed with the unglued stack can be used to determine the photoelectron yield for the glued stack prototype. The result is that ≈ 4 photoelectrons are observed for a single minimum ionizing particle. For comparison, the equivalent yield for a lead glass calorimeter is 70 photoelectrons.

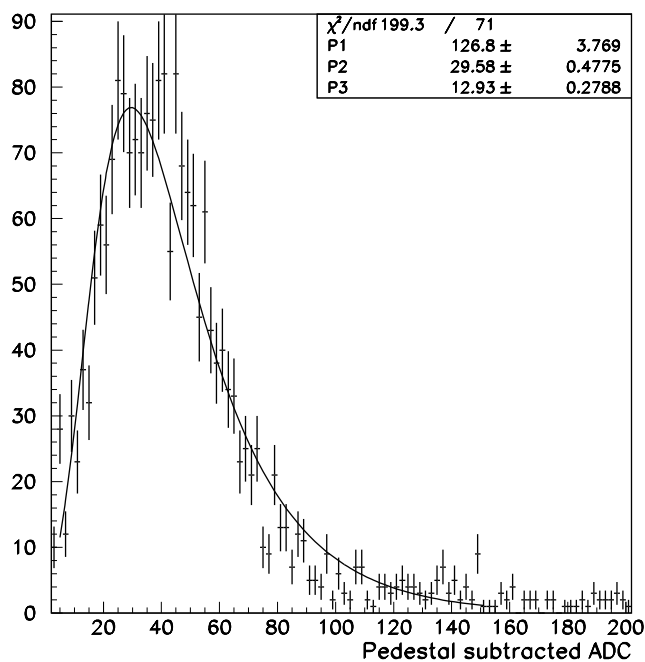


Figure 5: A typical ADC spectrum from the glued scintillator stack.

4.3 Attenuation length

The attenuation length of the glued and unglued stacks was determined by measuring the response of the stacks as a function of the position of the trigger counters along the length of the modules. Data was taken at the center of each stack, defined to be $x = 0$ and positions ± 20 cm from the center. To verify the repeatability of the measurements, the glued stack was measured twice. During the second measurement of the glued stack, one of the measurements was taken 30 cm from the center. This was done to determine if geometric effects associated with measurements near an end of the stack were important.

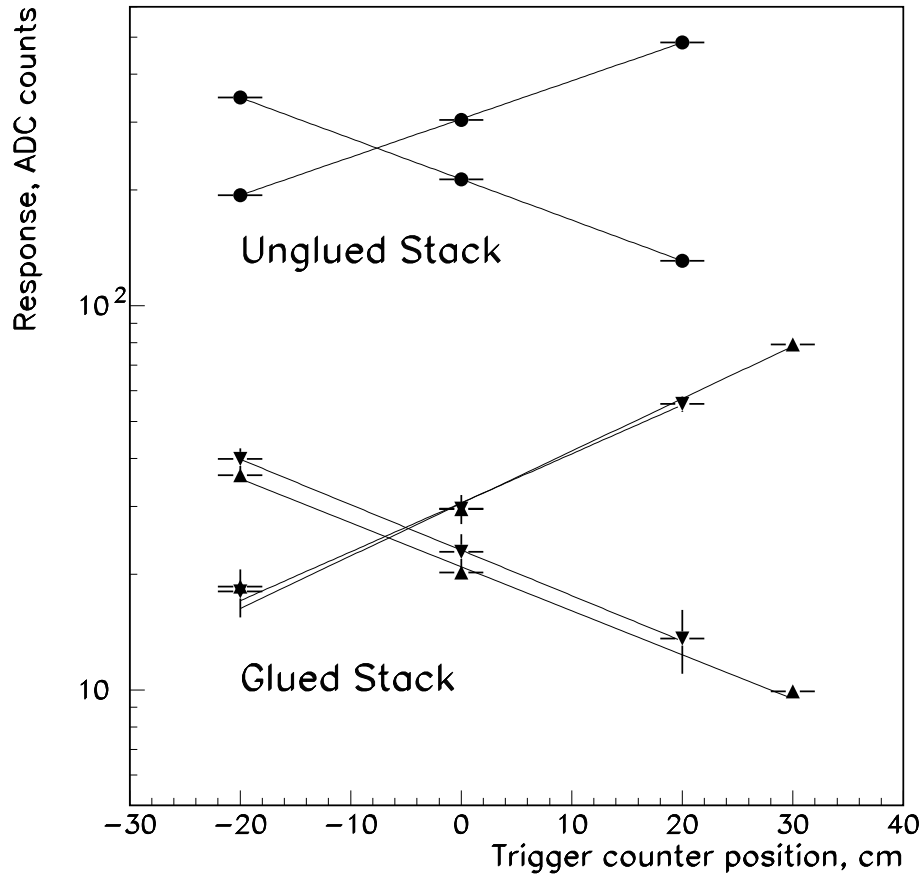


Figure 6: The results of the fits to the pulse height distributions for the unglued stack (top) and the glued stack (bottom) as a function of position.

Examination of figure ?? reveals several features of the data:

1. The measurements are repeatable, the different symbols shown for the glued stack represent the two different sets of data taken for that module
2. The attenuation lengths obtained for the glued and unglued modules are approximately equal
3. The light yield for the glued module is a factor of eight smaller for the glued module compared to the unglued module.

The lines shown if figure ?? are the result of a fit to

$$R(x) = R_0 \exp(-x/A). \quad (4)$$

The average attenuation length (A) obtained from all measurements was 37.5 cm . Variations between the measurements (from 31.8 to 43.7 cm) gives an estimated systematic error of $\pm 6 \text{ cm}$ on this measurement. A bulk attenuation length of 4 meters for this type of scintillator is claimed by the manufacturer. Previous measurements [?] for thicker (1.27 cm) slabs of this scintillator have given values for the attenuation length exceeding 2 meters. The significantly reduced value obtained here could be due to the increased number of reflections required to propagate the light to the phototubes. Any imperfections in the large surfaces of the scintillator would cause light loss even at angles consistent with total internal reflection. An attenuation length of less than 40 cm clearly precludes use of this technology in a 4 meter long calorimeter.

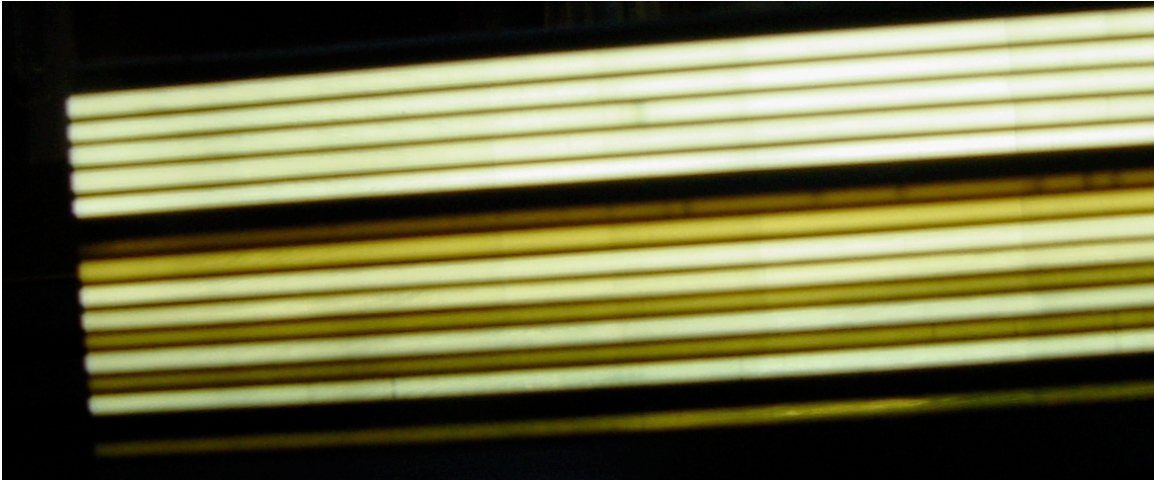


Figure 7: A closeup of an edge of the glued module. Light transmission has clearly been severely reduced in some layers.

The difference in total light yield between the glued and unglued modules is a factor of eight. Observation of the edge of the glued module (see figure ??) showed that several layers of the module produced no light. [†] The cause of this effect is not currently known, the same assembly

[†]Many other photographs of the module can be seen at
http://k9.physics.indiana.edu/eric/GlueX/1_meter/Module/index.shtml

techniques were used for all layers. Simple counting predicts this effect could account for a factor of two in light reduction. The remaining factor of 4 is most probably due to optical coupling of the scintillator to the lead. This would lead to a reduced angular acceptance for propagation of light by total internal reflection. In any case, the large reduction in light yield is a problem that would have addressed for this technology to be used in an operational detector.

5 Conclusions

The comparison of the glued and unglued stacks shows that scintillation light can be propagated down the length of the unglued scintillator sheets even given the non-parallel surfaces and the small thickness of the sheets. It also shows that the transmission mechanism is nearly destroyed by the process of bonding the lead to the scintillator. The existence of electromagnetic calorimeters based on SciFi technology with good resolution properties imply that the efficiency of transmission in fibers is very much higher than observed here.

It is concluded that manufacturing and performance limitations prevent using this technology without further R&D. In particular, methods to achieve

- 1) Full length scintillator sheets
- 2) Higher mechanical tolerances during casting
- 3) Better light transmission after gluing, possibly including cladding

would have to be developed for the technology studied here to be competitive with existing SciFi calorimeter technology. Since the savings associated with the technology investigated here are costs associated with assembly labor, expending effort associated with this R&D effort is probably not cost effective.

References

- [1] K. V. Aleksandrov *et al.*, Nucl. Instrum. Meth. A **459**, 123 (2001).
- [2] M. Incagli, AIP Conf. Proc. **450**, 437 (1998).
- [3] G. Basti *et al.*, Nucl. Phys. Proc. Suppl. **54B**, 210 (1997).
- [4] The GlueX Collaboration, GlueX-doc-346-v2, Unpublished.
- [5] S. Denisov *et al.*, Nucl. Instrum. Meth. A **525**, 183 (2004).